Bažant, Z.P. (1982) "Mathematical models of non- linear behavior and fracture of concrete." in *Nonlinear numerical analysis of reinforced concrete*, ed. by L.E. Schwer, Proc., ASME *Winter Annual Meeting*, held in Phoenix, Arizona, publ. by ASME, New York, pp. 1–25.

Nonlinear Numerical Analysis of Reinforced Concrete

presented at

THE WINTER ANNUAL MEETING OF
THE AMERICAN SOCIETY OF MECHANICAL ENGINEERS
PHOENIX, ARIZONA
NOVEMBER 14-19, 1982

sponsored by

THE APPLIED MECHANICS DIVISION, ASME
THE PRESSURE VESSELS AND PIPING DIVISION, ASME

edited by

LEONARD E. SCHWER
SRI INTERNATIONAL

THE AMERICAN SOCIETY OF MECHANICAL ENGINEERS
United Engineering Center 345 East 47th Street New York, N. Y. 10017

MATHEMATICAL MODELS OF NONLINEAR BEHAVIOR AND FRACTURE OF CONCRETE

Z. P. Bažant, Professor of Civil Engineering and Director
Center for Concrete and Geomaterials
Technological Institute
Northwestern University
Evanston, Illinois

ABSTRACT

A review of some non-classical mathematical formulations for the constitutive behavior and fracture of concrete is presented. After pointing out certain limitations of the orthotropic models, the plastic-fracturing theory and the endochronic theory are discussed. Attention is then shifted on internal friction and dilatancy, particularly in relation to the fundamental stability postulates and work inequalities. Some possibilities of modeling frictional phenomena due to oriented cracks are outlined, and finally the modeling of fracture by means of strain-softening constitutive relations is examined. Some typical comparisons with test data are given.

INTRODUCTION

Concrete, the most widely used material both in terms of tonnage and costs, is characterized by an extremely complicated microstructure which endows it with an equally complicated behavior. The microstructure consists of a random dense array of irregular large inclusions of a hard mineral, embedded within a softer and weaker matrix of mortar, which itself consists of small hard inclusions embedded within a still softer and weaker matrix of hardened portland cement paste. The bond between these inclusions (the pieces of aggregate and sand grains) and the matrix is relatively weak causing that microcracks begin to form at relatively small stresses, and that microcrack formation is the chief source of inelastic behavior, prevailing over plastic deformations.

In the present lecture, an attempt is made to review and summarize some mathematical models for the nonlinear inelastic behavior and fracture of concrete which were recently developed at Northwestern University. The literature on this subject has become vast, and the reader must be warned that no attempt is being made for a complete and balanced presentation of the state-of-the-art. For this purpose, some other works have recently become available (1).

ORTHOTROPIC MODELS

It may perhaps be of interest to begin by pointing out the limitations of the orthotropic models — an approach which has been most popular and most widely utilized in finite element programs. In these models, one assumes the incremental stress-strain relation to be linear, characterized by a tangential stiffness or compliance matrix that is of orthotropic form, with zero coefficients relating the normal strain increments to the shear stress increments. This simplification has the advantage that the variation of tangential elastic moduli or compliances can be to some extent figured out by direct intuitive reasoning, without the aid of more sophisticated concepts such as inelastic potentials, flow rule and normality, stability postulates, etc.

An orthotropic form of the tangential stiffness or compliance matrix is obviously correct only if the principal directions of stress and strain do not rotate. Problems arise in general loading situations in which these directions rotate. The orthotropic models can then be applied in two different ways:

1. Either the coordinate axes to which the material orthotropic properties are referred are kept fixed with regard to the material during the deformation process (although arbitrary coordinates may of course be introduced before deformation begins);

2. Or the axes of orthotropy are rotated during the deformation process (from one loading step to the next) so that they remain parallel to the principal stress directions at the beginning of each load step.

Consider the second method, which is probably used most often. The nonlinearity of the material response is due to formation of certain defects (e.g., microcracks as we consider them here, or slips) by the previous deformation history.

The rotation of the axes of orthotropy means that we rotate these defects against the material. This is of course physically impossible, and would be acceptable only if the defects were either caused solely by the current stress state (and not by the previous deformations) or if they had no oriented character (e.g., round voids rather than planar microcracks). Such an assumption is obviously unacceptable for geomaterials. In continuum mechanics of inelastic behavior it is a generally accepted fundamental fact that the material axes must remain fixed with regard to the material after the deformation begins. The symmetry properties, such as isotropy, are characterized by the fact that any coordinate axes may be chosen before the deformation begins, and the obtained responses must be equivalent. This however does not permit rotating the coordinate axes after the material has already been deformed.

Another problem with rotating the axes of material orthotropy appears when we consider the principal directions of strain. These rotate also, but in general, according to the orthotropic models as well as in reality, their rotations are not the same as those of the principal directions of stress. Therefore, the principal directions of stress and of strain cease to be parallel. Should then the material orthotropy axes be oriented parallel to the principal stress directions or to the principal strain directions? Evidently, they cannot be parallel to both.

Consider now the first method in which the material properties are described in terms of coordinate axes that are attached to the material as it deforms, and consider the constitutive relations

$$d\sigma_{ij} = D_{ijkm}(\underline{\sigma})\, d\epsilon_{km} \tag{1}$$

in which the tangential moduli tensor D_{ijkm} is a function of the stress tensor $\underline{\sigma}$. For isotropic (precisely, initially isotropic) materials, it must be possible to apply these relations for arbitrarily chosen coordinate axes and get equivalent results. Therefore, these incremental constitutive relations must be form-invariant under any transformation on the coordinate axes. This form-invariance condition is expressed mathematically in the form (see e.g., Malvern (2).

$$D_{pqrs}(\underline{\sigma}') = a_{pi}\, a_{qj}\, a_{rk}\, a_{sm}\, D_{ijkm}(\underline{\sigma}) \tag{2}$$

in which $a_{ij} = \cos(x_i', x_j)$ = the transformation tensor containing the directional cosines of the rotated axes x_i' with respect to the original axes x_j, and $\underline{\sigma}'$ is the stress tensor in the rotated system of coordinate axes x_i', obtained by the tensorial transformation of stress tensor $\underline{\sigma}$ in the original axes x_i; $\sigma'_{uv} = a_{ug}\, a_{vh}\, \sigma_{gh}$. It can be demonstrated (3) that the foregoing condition is always violated by the orthotropic incremental elastic models when they are applied using the first method. It can be also shown (3) that the lack of objectivity due to the lack of tensorial invariance can cause serious discrepancies, i.e., the predictions obtained when working with different coordinate systems can greatly differ, sometimes as much as 50%. (Note that the fact that after coordinate transformation the orthotropic matrix yields a matrix with non-zero coefficients relating normal strains and shear stresses is immaterial; this is because the orthotropic symmetry properties do not change with the coordinate transformation and apply after transformation with respect to the rotated axes.)

The use of a relation between total stresses and total strains does not suffer with the limitations of the orthotropic models. In fact, differentiations of such a stress-strain relation yields an incremental stiffness or compliance matrix which is, in general, fully populated, and is not of orthotropic form (with zeros in the elements connecting shear strains and normal stresses). This observation also shows that the assumption of irreversible defects and path-independence does not provide a justification for the orthotropic models, since it leads to the total deformation theory which is incompatible with these models.

The recent popularity of orthotropic stress-strain relations has no doubt been caused by the recent exaggerated emphasis on the cubic triaxial tests, as opposed to the classical cylindrical triaxial tests. In cubic specimens, the principal stress axes cannot be made to rotate during the loading process, and by virtue of symmetry the principal directions of stress and strain are forced to coincide. The cubic triaxial tests have of course the advantage that they can reveal the effect of the medium principal stress. In many situations this seems to be however less important than the knowledge or the effect of rotation of principal stress directions and the effect of non-coincidence of the principal stress and strain directions (the lack of coaxiality).

To be able to observe the effect of rotating principal stress directions, other types of tests will be needed. One such type of test is a classical test in which a hollow cylinder is subjected to axial load, lateral external and internal pressure, and torsion. In this test one can induce any combination of

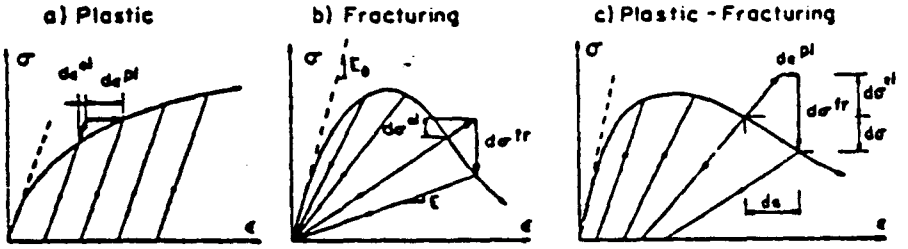

Fig 1. Idealized Unloading Behavior Imagined for Plastic-Fracturing Theory

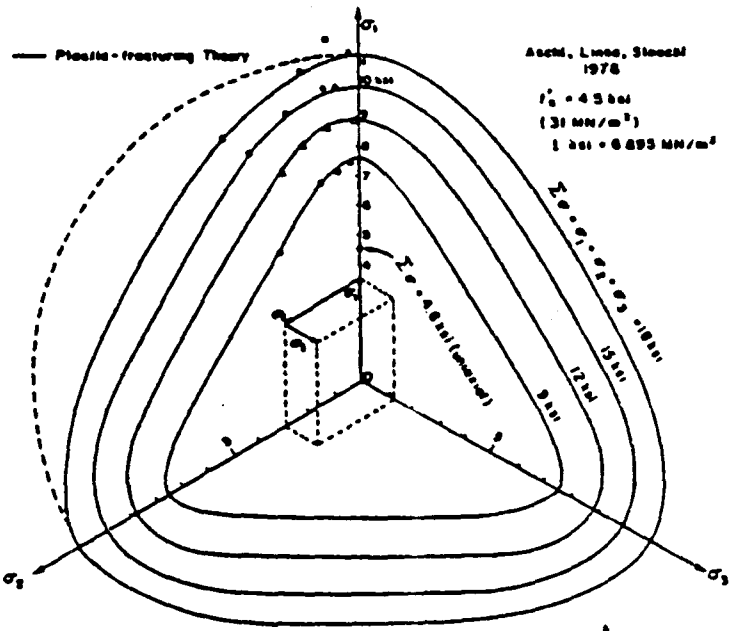

Fig. 2

Failure envelopes obtained from plastic fracturing theory, the loading surfaces of which do not involve third invariants of stress and strain

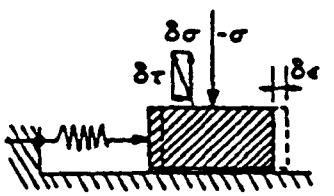

Fig. 4 Example of a Spring-Loaded Frictional Block

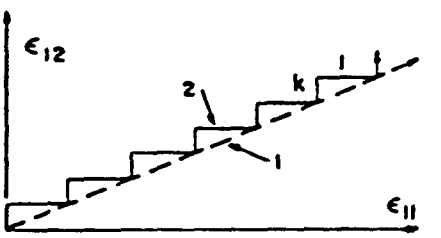

Fig. 3. Staircase Loading Path

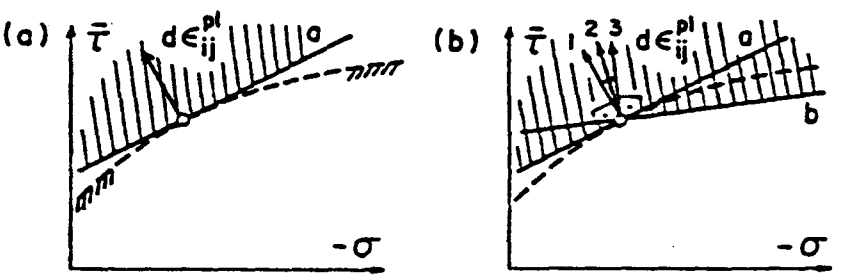

Fig. 5

Plastic Strain Increment Relative to Loading Surface

principal stresses, and moreover one can make the principal stress directions have any angle with the specimen axis and rotate, either continuously or abruptly, during the loading process. Much more attention should be given to this type of test in the future.

PLASTIC-FRACTURING THEORY

Since the major source of inelastic behavior in concrete is microcracking rather than plastic slip, applications of the theory of plasticity to concrete do not appear to be physically justified. Other theories, which in some way take the phenomenon of microcracking into account are therefore appropriate. One such theory is the plastic-fracturing theory. This theory represents an extension of classical incremental plasticity (4) which adheres to the use of loading surfaces and flow rule based on these surfaces, and introduces, in addition to plastic strain increments, the fracturing stress relaxations due to microfracturing (microcracking). The extension to model the inelastic phenomena due to microcracking appears to be essential for materials such as concrete as well as rocks (5-6).

The nature of the theory may be illustrated by Fig. 1, in which plasticity is seen to be characterized by an elastic increment followed by a horizontal plastic strain increment. A material which undergoes only microfracturing and no plastic deformation, first studied by Dougill (7-8), is shown in Fib. 1b where the elastic increment is followed by a vertical fracturing stress decrement. While plasticity obviously does not allow strain-softening, i.e., decline of stress at increasing strain, the fracturing theory does. To be able to distinguish strain softening from unloading, the unloading surfaces for the fracturing theory must be considered as functions of strains rather than stresses, as was first done by Dougill (7-8), who also introduced the normality rule in the strain space to obtain fracturing stress relaxations. The plastic-fracturing theory is a combination of plastic and fracturing theories and is illustrated in Fig. 1c, where the elastic increment is followed by a horizontal plastic strain increment and then by a vertical fracturing stress decrement. Obviously, the strain softening is also allowed in this theory. The plastic strain increments and fracturing stress decrements are then obtained on the basis of separate loading surfaces in the stress and strain spaces (5-6).

The characteristic property which allows us to distinguish between plastic and fracturing phenomena is the unloading slope. The plastic phenomena do not lead to any change in the unloading stiffness, while the fracturing phenomena are totally related to a change in the unloading stiffness, and in case of pure fracturing behavior they preserve total reversibility at complete unloading, as indicated by the fact that the unloading slope in Fig. 1b shoots to the origin. In plastic-fracturing materials (Fig. 1c) the unloading slope decreases but does not point to the origin. If the unloading slope is known for each point of the loading diagram, it is possible to uniquely separate the plastic and fracturing effects (6).

The plastic-fracturing theory leads to the following incremental stress-strain relations (5):

$$ds_{ij} = 2G de_{ij} - 2G s_{ij} \frac{du}{\tau} - e_{ij} \frac{d\kappa}{\gamma} \tag{3}$$

$$d\sigma = 3K d\varepsilon - 2K \beta \, du - \frac{2}{3} \alpha d\kappa \tag{4}$$

in which

$$d\kappa = H_1(d\bar{\gamma} + \alpha' d\varepsilon), \quad d\mu = H_2(Gs_{km}d\varepsilon_{km} + \bar{\tau}K\beta' d\varepsilon_{kk}) \tag{5}$$

Here, G = elastic shear modulus, K = elastic bulk modulus (both moduli are variable); s = deviator of stress tensor σ_{ij}, e_{ij} = deviator of strain tensor ε_{ij}; σ = mean (hydrostatic) stress, ε = mean (volumetric) strain = $\varepsilon_{kk}/3$; μ, κ = parameters for plastic and fracturing deformation; $\bar{\tau}$ = stress intensity, $\bar{\gamma}$ = strain intensity = $(e_{ij}e_{ij}/2)^{\frac{1}{2}}$; β', α' = plastic and fracturing internal friction coefficients; β, α = plastic and fracturing dilatancy factors giving the ratio of volumetric to deviatoric inelastic increments; and H_1, H_2 = hardening and softening stiffnesses. The inelastic response is here totally characterized by six coefficients, H_1, H_2, β', α', β, α, the dependence of which on the invariants of stress and strain must be determined from experiment. Various other considerations are needed for this purpose and suitable functions for these coefficients have been identified, leading to a rather close agreement with a broad range of experimental data available in the literature (see Ref. 5).

In constrast to incremental plasticity, the constitutive equations of plastic fracturing theory (Eqs. 3-5) involve not only terms which depend on stress (the term with s_{ij} in Eq.3), but also terms which depend on strains such as the term involving e_{ij} in Eq.3 . These terms appear to be very helpful in representing material behavior in strain-softening regimes, which is due simply to the fact that e_{ij} increases during strain-softening while s_{ij} decreases. These strain-dependent terms give rather different lateral strains and thus allow us to model the large volume dilatancy during strain-softening.

Another essential difference from plasticity is that the shear and bulk elastic moduli are variable. Their decrease is tied to the growth of fracturing parameter κ, for which the following equations were obtained (5):

$$dG = \frac{d\kappa}{2\bar{\gamma}} \qquad dK = -\frac{2\alpha}{9}\frac{d\kappa}{\varepsilon} \tag{6}$$

Note that Eq. 3 applies only to loading; for unloading modified expressions must be introduced. In analogy to plasticity, one might set $d\kappa = d\mu = 0$, but then no representation of inelastic behavior on unloading, reloading and cyclic loading would be possible. It is possible, however to formulate rules which allow for nonzero $d\kappa$ and $d\mu$ during unloading and cyclic loading (5). These rules consist in the so-called jump-kinematic hardening, in which the center of the loading surface is jumped to the last extreme stress or strain point whenever loading is reversed to unloading or vice versa. Three-way loading-unloading-reloading criteria are needed for this purpose (5).

The most important advantage of the plastic-fracturing theory is the fact that the stress-strain relationships (Eqs. 3-5) can be brought (for loading) to an incrementally linear form:

$$d\sigma_{ij} = C_{ijkm}(\underset{\sim}{\sigma}, \underset{\sim}{\varepsilon})d\varepsilon_{km} \quad \text{or} \quad d\underset{\sim}{\sigma} = C(\underset{\sim}{\sigma}, \underset{\sim}{\varepsilon})d\underset{\sim}{\varepsilon} \tag{7}$$

in which C_{ijkm} or $\underline{C}$ represent the tensor or matrix of the tangential moduli which are functions of the invariants of the stress tensor $\underline{\sigma}$ and strain tensor $\underline{\varepsilon}$; see Ref. 5. The use of tangential moduli is the most effective approach in step-by-step finite element analysis.

Observe that the matrix of tangential moduli is non-symmetric. This is a consequence of internal friction and is inevitable for close representation of experimental data on the material behavior. This is certainly an inconvenience for numerical finite element analysis. However, it must be emphasized that this type of non-symmetry does not cause material instability as long as the inequality given below in Eq. (12) is satisfied. It should be also noted that tangential moduli C_{ijkm} have a generally anisotropic (non-isotropic and non-orthotropic) form, which is a manifestation of the stress- and strain-induced anistropy.

The stress-strain relations in Eqs. 3-5 were derived by using loading surfaces that do not involve the third invariants of stress and strain. It is, however, interesting that the failure envelopes obtained from these relations (by recording the peaks of the stress-strain diagrams run at various fixed ratios of of stress components) have a shape that is non-circular on the octahedral plane (π - projection). This is illustrated by the diagram in Fig.(2) which was constructed from the numerical values of the coefficients of the plastic-fracturing theory as given in Ref. (5). This shows that the rounded triangular shape of the octahedral section does not necessarily imply the influence of the third stress invariant. This shape can be equally well explained by the simultaneous influence of stress and strain on the failure surface and the fact that the strains do not increase proportionally to stresses.

The plastic-fracturing theory has been shown to be capable of representing a very broad range of inelastic phenomena. These include: Strain-softening, inelastic dilatancy due to shear and internal friction, as manifested by the great effect of hydrostatic strength in triaxial tests, the increase of volume in pre-peak as well as post-peak deformation, lateral strains, the increase of apparent Poisson ratio, hysteretic loops during cyclic loading to small as well as high strength levels, etc. (data from Refs. 9-15 fitted in Ref. 5).

ENDOCHRONIC THEORY

Another theory which has met with considerable success in modeling the observed material behavior is the endochronic theory. The general framework of this theory was developed by Valanis (16), although an elementary prototype of this approach had been suggested earlier (17). The central concept in this theory is that of the intrinsic time, which is a variable which depends on the length of the path traced by the states of the material in the strain space. The original Valinis definition of the intrinsic time, z, which was used for concrete, is:

$$dz = F_1(z, \underline{\sigma}, \underline{\varepsilon})\, d\xi, \quad d\xi = \sqrt{\frac{1}{2} de_{ij} de_{ij}} \tag{8}$$

in which F_1 is a function of the stress and strain invariants and models the hardening or softening of the material during the evolution of inelastic strain. The inelastic strain increments are assumed to be proportional to dz and the constitutive relation of endochronic theory has the following form (26,27):

$$de_{ij} = \frac{ds_{ij}}{2G} + \frac{s_{ij}}{2G}\, dz, \qquad d\varepsilon = \frac{d\sigma}{3K} + d\lambda \tag{9}$$

Here an additional term, called inelastic dilatancy, $d\lambda$, is introduced to model the inelastic dilatancy due to shear. This term is also related to intrinsic time:

$$d\lambda = F_2(z, \underline{\sigma}, \underline{\epsilon})d\xi \tag{10}$$

It can be shown that the endochronic theory is a special case of visco-plasticity in which the viscosity coefficients depend not only on stress and strain but also on the strain rate (8).

The chief advantage of the endochronic theory, first recognized by Valanis, is the fact that it is capable of representing the unloading irreversibility, the salient feature of inelastic behavior, without the use of any inequalities (unloading criteria). This makes the endochronic theory extremely effective for cyclic loading. Furthermore, the fact that all inelastic strains are tied to one time-like variable dz makes it easy to control the stiffening or softening of the material by changing the rate of growth of the intrinsic time. One aspect which is particularly easily modeled by the theory is the inelastic volume dilatancy $d\lambda$.

The most significant difference of the endochronic theory from classical plasticity as well as plastic-fracturing theory is the fact that, even for loading, it cannot be reduced to an incrementally linear form given by Eq. (7). Nevertheless, in the vicinity of any specified loading direction the endochronic theory can be linearized, i.e., brought into an incrementally linear form (18). However, the tangential moduli C_{ijkm} of this linearized form are not constant and depend on the chosen direction in the vicinity of which the behavior is linearized.

It may seem that the lack of incrementally linear formulation would cause significant difficulties in numerical computation. However, finite element programs utilizing endochronic theory have been written (e.g., 19-23), and no particular convergence difficulties have been encountered.

Endochronic theories have recently been criticized from the viewpoint of material stability and uniqueness of response (24-25). Subsequently, it was shown, however, that the theory can be either modified to satisfy these requirements, for example by the use of jump-kinematic hardening and by unloading- reloading criteria (18,27), or that the strong uniqueness requirements are themselves in question. For example, Rivlin (24) pointed out that when one considers a staircase loading history in the strain space (Fig. 3) and when one lets the size of the stairs shrink to zero and their number goes to infinity, the limiting behavior does not approach that for the smooth loading path. It is, however, possible to formulate a refined definition of intrinsic time (intrinsic time with finite resolution) for which the limit coincides (6), although at the same time the need for doing this may be questioned because the staircase loading path might not cause the same type of damage to the material as does the smooth loading path.

The comparisons with available test data have been very successful, about equally good with the endochronic theory and the plastic-fracturing theory (27). One might thus wonder why two rather different theories allow representation of the same phenomena. The answer is that our information on the material behavior is far from complete and is insufficient to completely define the mathematical formulation. Therefore, certain logical assumptions must inevitably be used and the resulting formulation also depends on these. It appears that the most significant difference between various theories of inelastic behavior is obtained when a proportional loading is followed by sudden load increments to the

side of the previous loading path; e.g., when an increase of normal stress is followed by a sudden shear stress increment. The different responses for such loading may be graphically illustrated in terms of the inelastic stiffness locus (18). It is unfortunate that for such loading paths measurements are most difficult and the present experimental information is rather scant. However, improvement of our knowledge for this type of loading is important because the loading "to the side" is characteristic of failures due to material instability.

INTERNAL FRICTION AND DILATANCY

An important aspect of the physical mechanism of inelastic response of concrete is, no doubt, the frictional slip of the surfaces of closed microcracks. Friction causes a major complication in constitutive modeling since it leads to violation of the basic stability postulate, namely Drucker's postulate (38,39), which serves as the basis for the flow rule (normality rule). The postulate is given by the inequality

$$\Delta W = \frac{1}{2} d\sigma_{ij} d\epsilon_{ij}^{p\ell} > 0 \tag{11}$$

in which ΔW represents the second-order work dissipated during a cycle of applying and removing stress increments $d\sigma_{ij}$, and $d\epsilon_{ij}^{p\ell}$ are the increments of plastic strains. This postulate is known to represent a sufficient but not necessary condition for local stability of the material (27a, 28, 2, 6). It is important to realize that its violation does not necessarily imply instability. In fact, certain conditions under which this postulate may be violated yet stability is still guaranteed has been recently formulated (6) extending previous analysis by Mandel (29). The following more general inequality which guarantees stability of the material has been found (6):

$$\Delta W - \chi \Delta W_f > 0 \tag{12}$$

in which χ is a parameter which can have any value between 0 and 1. Drucker's postulate is obtained for $\chi = 0$. The quantity ΔW_f represents a second-order energy expression defined as

$$\Delta W_f = \frac{\beta' - \beta^*}{2C} d\sigma(d\bar{\tau} + \beta^* d\sigma) \tag{13}$$

which may be called the frictionally blocked elastic energy. The material parameters in Eq. 11 are defined as

$$C = -k_1 \frac{\partial F/\partial \hat{\gamma}^{p\ell}}{\partial F/\partial \bar{\tau}}, \quad \beta' = \frac{\partial F/\partial \sigma}{\partial F/\partial \bar{\tau}}, \quad \beta^* = k_2 \frac{d\epsilon^p}{d\hat{\gamma}^{p\ell}} \tag{14}$$

where

$$F(\sigma, \bar{\tau}, \hat{\gamma}^{p\ell}) = 0 \tag{15}$$

represents the loading function of the material. The variable σ represents the mean (hydrostatic) stress, $\bar{\tau}$ is the stress intensity (square root of the deviator of the strain tensor ϵ_{ij}), and $\hat{\gamma}^{p\ell}$ is the length of the path traced in the space of plastic strains, which is used as a hardening parameter.

The meaning of the material parameters in Eq. 14 may be illustrated taking recourse to Mandell's example (29) (Fig. 4). A frictional block, resting on a rough horizontal surface is considered loaded by a vertical force simulating

the hydrostatic stress σ, and is also subjected to force F from a horizontal spring such that the *sliding* of the block is imminent. A horizontal force applied on the block simulates dF. Mandel *showed that* if a disturbing force $d\sigma_{ij}$ inclined from the vertical to the left by an angle less than the friction angle is applied (Fig. 4), the block is caused to slide but since the displacement to the right is infinitesimal, *the initial* equilibrium state of the block is *stable*. Yet, Drucker's postulate (Eq.1) is violated for this displacement. Inequality (12) is not violated. Coefficient C from this inequality represents the spring constant, coefficient β' is the friction *coefficient* of the block, and β* is the *dilatancy* angle indicating the ratio of lifting of the block to its sliding.

The new generalized *condition* sufficient for material stability (Eqs. 12-13) makes it possible to formulate a frictional constitutive relation and check whether such a *relation* satisfies stability conditions. Moreover, by following the same line of reasoning as in classical incremental plasticity, one can derive the flow rule associated with this inequality. Such an analysis shows (6) that this flow rule *allows* certain, but not arbitrary, violations of the normality rule. It is found, for example, that in *the plane* of $\bar{\tau}$ vs. σ the admissible load increment vectors can deviate from the normal to the right and fill a fan of directions, the limiting inclined direction being uniquely determined by the loading surface (Fig. 5). The resulting flow rule *is*, however, completely different *from* that for non-associated plasticity because a single loading surface is used, and because, in contrast to non-associated plasticity, stability of the material is guaranteed.

Inequality (12) pertains only to the friction in deviatoric deformations caused by hydrostatic *compression*. It is possible to derive a more general inequality (4) which also involves the friction in volume change caused by deviator shear stress, a phenomenon which may be called the inverse friction. Further generalizations are possible when, in addition to loading surfaces *(potentials)* in the stress space, one also uses loading *surfaces in the* strain space.

TENSILE STRAIN-SOFTENING AND FRACTURE

We turn now attention to the modeling of the progressive formation of microcracks all the way *to complete* fracture. This obviously has a connection to fracture mechanics. However, it has been well demonstrated that the classical, linear fracture mechanics is not applicable to concrete except for structures of extremely large sizes *(e.g., dams)*. Some improvement is possible with the use of ductile fracture mechanics, however, the *assumptions* of this approach, namely extensive plastic yielding at the front of fracture, are clearly not applicable to concrete. The characteristic feature of the fracture formation in heterogeneous brittle materials such as concrete, as well as rocks, is the existence of a large *fracture* process zone in which the fracture forms through progressive microcracking. In typical situations of concrete structures, this zone *is not* of negligible size compared to the dimensions of the structures. We will now briefly outline a model which has been recently developed to describe such fracture processes and has been shown to be capable of very close representation of the *available* fracture test data for concrete as well as rock (11).

Consider progressive formation of microcracks caused by stresses σ_x, σ_y, σ_z, the *principal* directions of which remain fixed. Let the normal stress and strain components be grouped into the column matrices $\underline{\sigma} = (\sigma_y, \sigma_z, \sigma_x)^T$, $\underline{\varepsilon} = (\varepsilon_y, \varepsilon_z, \varepsilon_x)^T$, where T denotes the transpose, and $\varepsilon_x, \varepsilon_y, \varepsilon_z$ are the normal strains, assumed to be linearized, or small. The elastic stress-strain relation for the normal stress and strain components may be considered as $\underline{\sigma} = \underline{D}\,\underline{\varepsilon}$ or $\underline{\varepsilon} = \underline{C}\,\underline{\sigma}$,

in which

$$\underline{D} = \begin{bmatrix} D_{11} & D_{12} & D_{13} \\ & D_{22} & D_{23} \\ \text{sym.} & & D_{33} \end{bmatrix} \tag{16}$$

and

$$\underline{C} = \underline{D}^{-1} = \begin{bmatrix} C_{11} & C_{12} & C_{13} \\ & C_{22} & C_{23} \\ \text{sym.} & & C_{33} \end{bmatrix} \tag{17}$$

Here $\underline{D}$ and $\underline{C}$ represent the stiffness and compliance matrices of the uncracked material.

To figure the changes in the foregoing matrices caused by progressive microcracking, it is helpful to recall first the stiffness matrix of a fully cracked material, i.e., an elastic material which is intersected by continuously distributed (smeared) cracks normal to axis z; see e.g., Suidan and Schnobrich (31). This stiffness matrix is known to have the form:

$$\underline{D}^{fr} = \begin{bmatrix} D_{11} - D_{13}^2 D_{33}^{-1}, & D_{12} - D_{13} D_{23} D_{11}^{-1}, & 0 \\ & D_{22} - D_{23} D_{33}^{-1}, & 0 \\ \text{sym.} & & 0 \end{bmatrix} \tag{18}$$

This matrix is derived from the condition that the stress normal to the cracks must be zero and that the material between the cracks has the properties of an uncracked elastic material. This last assumption is, of course, a simplification, since often the material between continuous cracks may be damaged by presence of discontinuous microcracks which formed before the continuous cracks were produced.

Comparing the matrices in Eq. 16 and 18, we see that each element of the stiffness matrix is affected by cracking. Thus, modeling of a continuous transition from Eq. 16 to Eq. 18 would not be easy since each term of the stiffness matrix would have to be considered a function of some parameter of cracking. It appears however (30) that the situation becomes much simpler if one uses the compliance matrix $\underline{C}$. In that case one needs to consider only one element of the compliance matrix to change

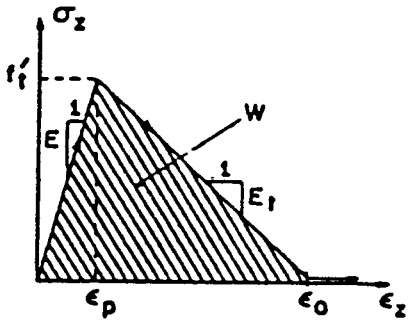

Fig. 6

Uniaxial Stress-Strain Relation Used in the Present Non-Linear Fracture Model

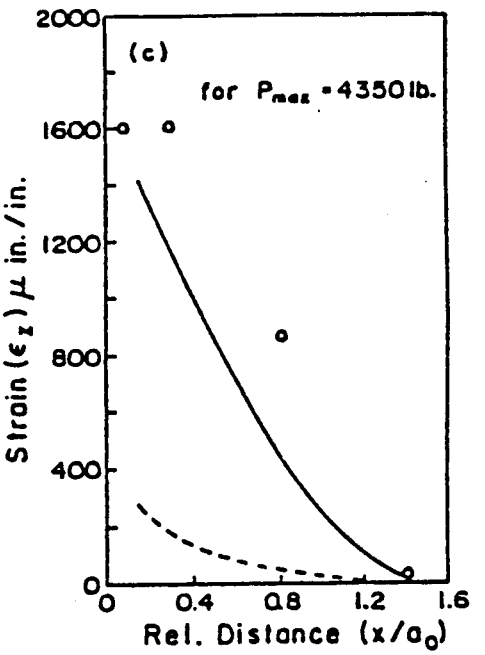

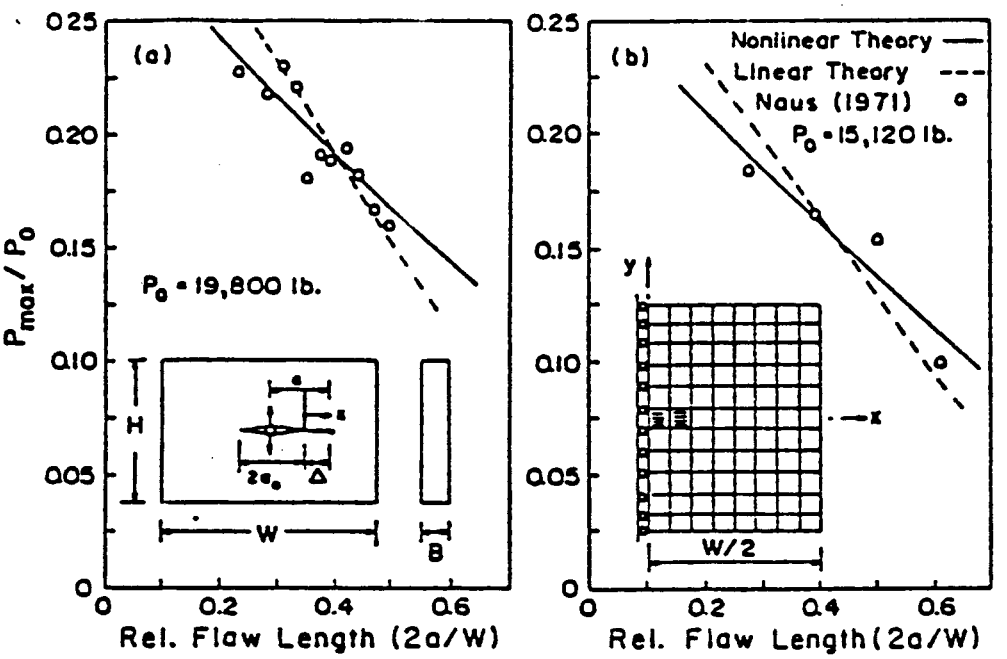

Fig. 7. Comparison With Maximum Load Data of Naus (1971) (after Bažant and Oh, 1981).

$$\underset{\sim}{C}(\mu) = \begin{bmatrix} C_{11} & C_{12} & C_{13} \\ & C_{22} & C_{23} \\ \text{sym.} & & C_{33}\mu^{-1} \end{bmatrix} \tag{19}$$

in which μ is a certain cracking parameter. There are two reasons for the effect of cracking on the compliance matrix to have this simple form:

1. If we assume all microcracks to be perfectly straight and normal to axis z, which is of course a simplification (in reality the microcrack orientations exhibit a certain statistical distribution), then formation of the microcrack has no effect on stresses σ_x and σ_y in the directions parallel to the crack planes. Therefore, appearance of microcracks normal to z should have only the effect of increasing the strain in the z direction, which is why, under this assumption, only the third diagonal term in Eq. 19 should be affected.

2. The second reason is that, in the limit $\mu \to 0$, the inverse of the compliance matrix in Eq. 19 is identical to the stiffness matrix of the fully cracked material in Eq. 18, i.e.,

$$\underset{\sim}{D}^{fr} = \lim_{\mu \to 0} \underset{\sim}{C}^{-1}(\mu) \tag{20}$$

This relation (theorem) has been proven mathematically (30) writing the general inverse of Eq. 19 with the help of partitioned matrices. It is also physically obvious that the diagonal compliance term for a fully cracked material should approach infinity because the material has no stiffness in the direction normal to the cracks and a finite stress therefore produces an infinite strain.

The use of Eq. 19 instead of Eq. 18 in finite element programming saves programmer's effort, since only one element of the elastic compliance matrix needs to be changed. In practice one may replace C_{33} by a large number (say 10^{40}), and numerical matrix inversion then yields a matrix nearly exactly equal to Eq. 16.

The cases of an uncracked and a fully cracked material are characterized, in terms of the cracking parameter, as follows:

$$\begin{aligned} &\text{uncracked:} \quad \mu = 1 \\ &\text{fully cracked:} \quad \mu = 0 \end{aligned} \tag{21}$$

Modeling of a progressive development of microcracks now obviously requires prescribing the variation of cracking parameter μ between these two limits (Eq. 21). The variation of this parameter may be calibrated on the basis of a uniaxial tensile test. From tests of small samples in an extremely stiff testing machine, e.g., Evans and Marathe, 1968 (32), it is known that the tensile stress-strain diagram exhibits a gradual decrease of strain at increasing strain (strain-softening), the softening branch being normally a few times longer than the rising branch. Although this tensile stress-strain relation appears to be smoothly curved, it may be approximated by a bilinear stress-strain relation (Fig. 6). In such a case the cracking parameter is defined as

$$\mu^{-1} = \frac{-C_{33}^{t}}{C_{33}} \frac{\epsilon_z}{\epsilon_0 - \epsilon_z} \tag{22}$$

in which C_{33}^{t} is the downward slope of the softening portion of the tensile stress-strain diagram (negative), and ϵ_0 is the tensile strain in uniaxial tensile tests at which the stress is reduced to 0, i.e., continuous cracks form.

Eq. 22 for the bilinear tensile stress-strain diagram may be easily replaced by a more complicated equation corresponding to a curved tensile stress-strain diagram. However, it appears that the bilinear stress-strain diagram is sufficient to obtain a satisfactory agreement with existing test data on fracture. Moreover, the use of a straight-line strain-softening diagram avoids uncertainty with the point at which unstable strain localization leading to fracture appears.

The foregoing stress-strain relations involve only the normal stress and strain components. They are obviously applicable only when the principal stress directions do not rotate during the formation of fracture. Even then, if the loading subsequent to fracture formation produces shear strains on the crack planes, the stress-strain relation must be expanded by the inclusion of shear terms (leading to a 6 x 6 stiffness or compliance matrix).

Another adjustment of the foregoing stress-strain relation is appropriate when there are significant compressive normal stresses in the directions parallel to the crack plane. In such a case it is necessary to decrease the value of the peak stress f_t' as a function of σ_x and σ_y (30).

Finally, note that then there is certainly a similarity between the present stress-strain relation and the stress-displacement relation used in other works (33-39).

An essential aspect in modeling fracture by strain-softening stress-strain relations is to realize that the width of the crack band front must be considered as a material property. There are very definite theoretical reasons for this.

1. If the crack band width is considered as a variable, and the material is treated as a continuum, then an analysis of the strain-localization instability indicates that the crack band would always localize to a sharp front of vanishing width. This situation is however equivalent to linear fracture mechanics and cannot describe the test data available for rock and concrete.

2. It is meaningless to consider the crack band front to be less than a few times the size of the heterogeneties in the material, such as grain size in rock (or aggregate size in concrete). On such small dimensions one does not have a continuum, and the foregoing continuum model would be inapplicable.

3. Finally, the mathematical model must satisfy the conditions of objectivity,* which includes the requirement that the results of analysis must be independent of analyst's choice of the mesh (except for an inevitable numerical error which vanishes as the mesh is refined). It has been verified numerically that if the width of the finite element over which the crack band is assumed to be distributed is varied, the fracture predictions vary too. The only way to achieve consistent results is to assume that the width of the crack band at the fracture front is fixed.

*Refs. 40,41

Modeling of fracture by means of stress-strain relations thus leads to a model characterized by three material parameters: the uniaxial tensile strength, f'_t, the fracture energy G_f (defined as the energy consumed by crack formations per unit area of the crack plane), and the width w_c of the crack band front. Since

$$G_f = W_f w_c \tag{23}$$

where W_f is the work of the tensile stress per unit volume, equal to the area under the tensile stress-strain diagram (Fig. 6), the softening slope C^c_{33} is not an independent parameter and follows from the values of f'_t, G_f, and w_c.

The foregoing simple stress-strain relation for tensile strain-softening has been implemented in a finite element program. For this purpose, the stress-strain relation is differentiated and used in an incremental loading analysis.

FITTING OF TEST DATA AND VERIFICATION

Most of the important test data from the literature (42-57) have been successfully fitted in report (30) with the present nonlinear fracture model. Some of the fits from Ref. (30) are shown in Figs. 7-10 by the solid lines. The best possible fits obtainable with linear fracture mechanics are shown for comparison in these figures as the dashed lines. The fits were calculated by the finite element method using square meshes. The loading point was displaced in small steps and the response of the specimen was calculated in small loading increments. The *same* stress-strain relation, as indicated before, was assumed to hold for all finite elements. However, only some elements entered nonlinear behavior. A plane stress state was assumed for all calculations. The preceding stress-strain relations were differentiated and converted to an incremental form for the purpose of step-by-step loading analysis.

In fitting these test data, it was discovered that the optimum width on the crack band front was for all cases between 2.5 and 4-times the maximum aggregate size and, furthermore, the crack band front width

$$w_c = 3d_a \tag{24}$$

was nearly optimum for all calculations (d_a = maximum aggregate size). It was for this width w_c that the area under the stress-strain curve yielded the correct value of the fracture energy needed to obtain good fits of the test data. It thus appears that, at least for plain concretes, the width of the crack band front may be easily predicted from the maximum aggregate size. However, we must caution that the foregoing simple relation might not hold for high strength concretes, in which the fracture seems to be more brittle, the crack band more concentrated.

In view of Eq. 22, the fracture theory presented in this lecture is essentially a two-parameter theory, the two material parameters to be determined by experiment being G_f and f'_c.

The aforementioned analyses of test data involved the maximum load tests, as well as tests of the resistance curves (R-curves), in which the apparent fracture energy is determined as a function of the crack extension from a notch.

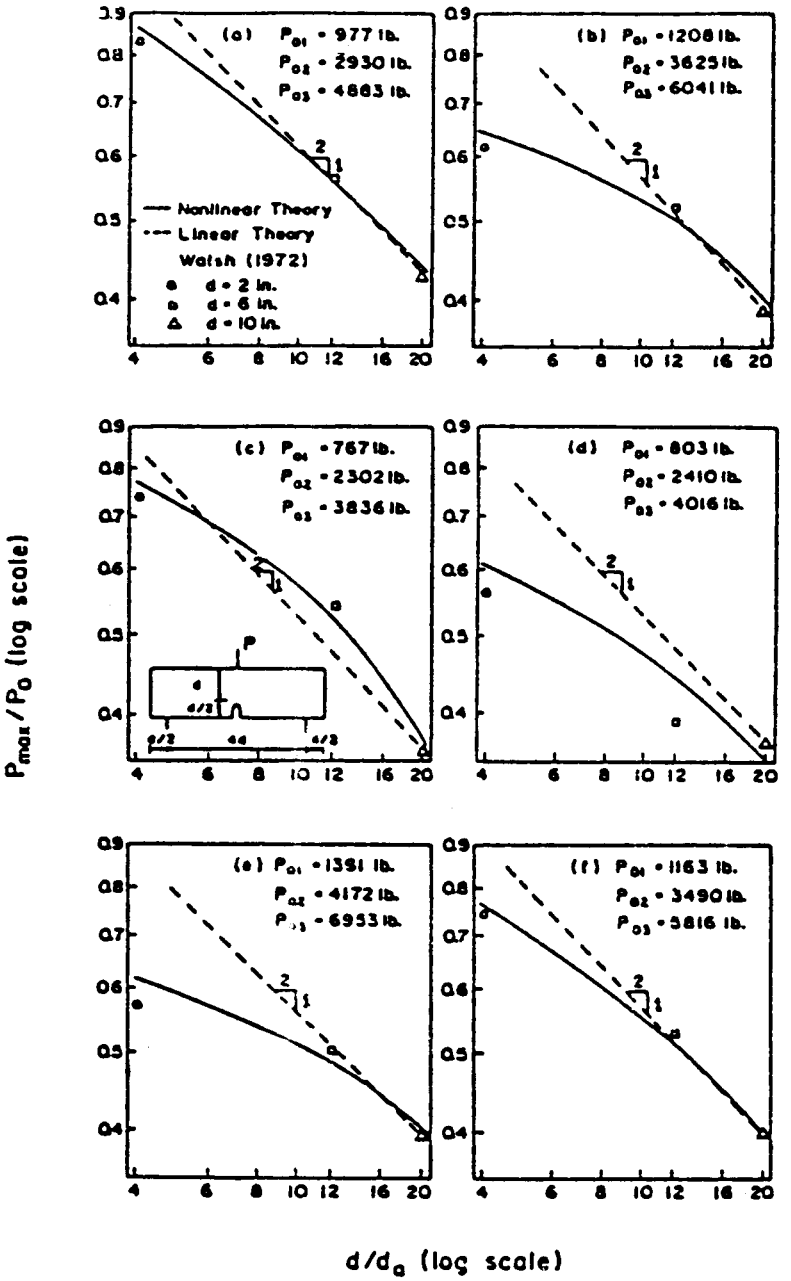

Fig. 8. Comparison With Maximum Load Data of Walsh (1972, for Six Different Concretes. (after Bažant and Oh, 1981).

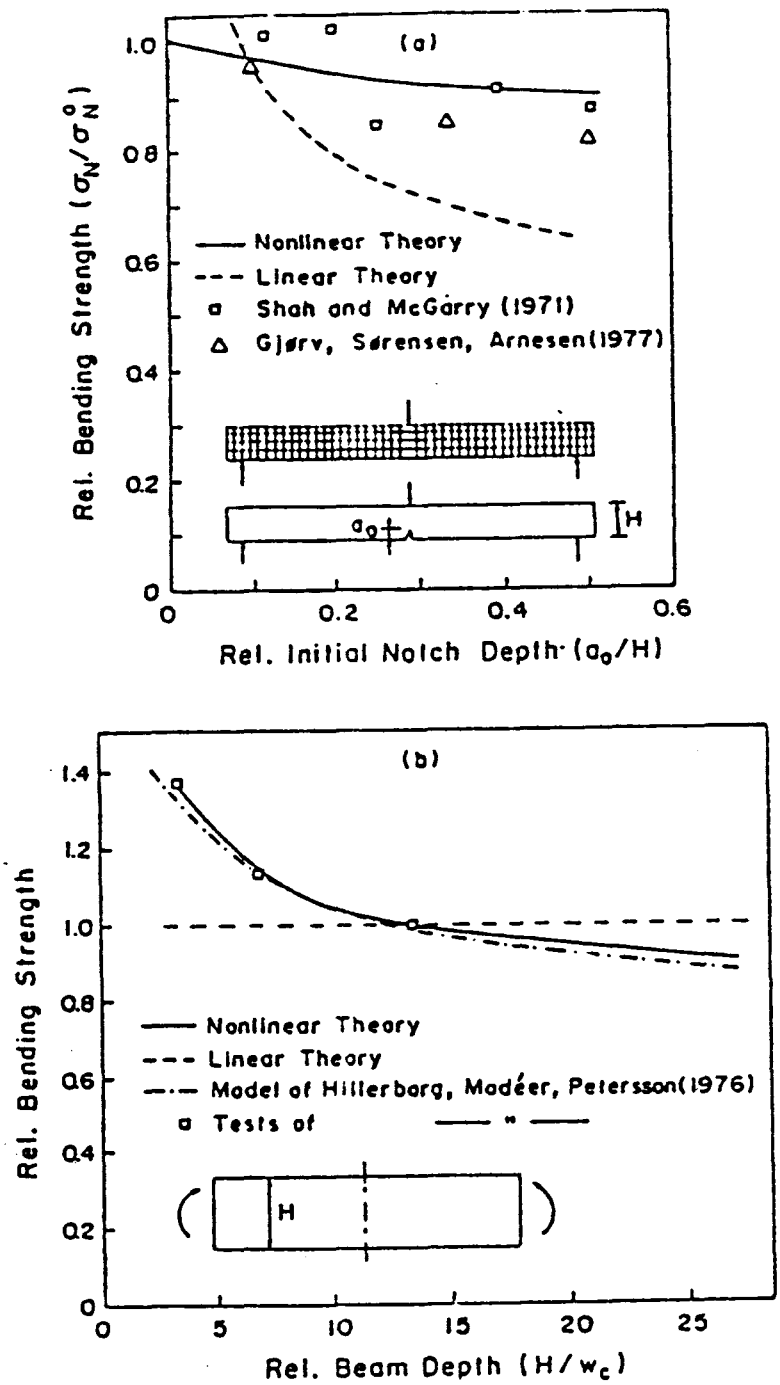

Fig. 9. Comparison With Maximum Load Data of Shah and McGarry (1971), Gjørv et al. (1977) and Hillerborg et al. (1976) (after Bažant and Oh, 1981).

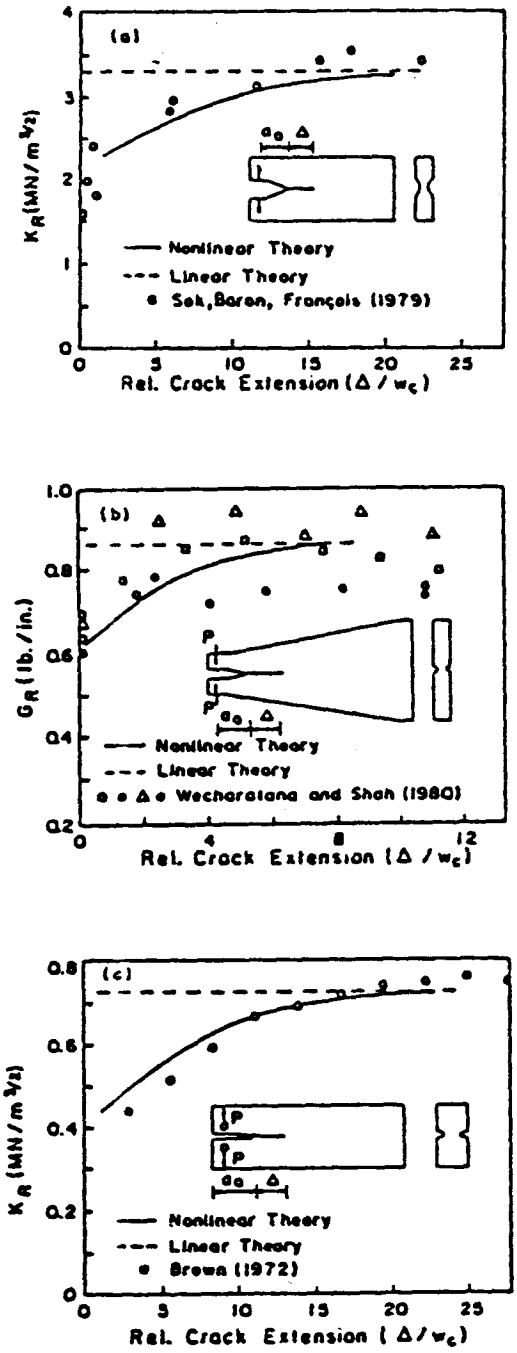

Fig. 10. Comparisons With Resistance Curve Data of Sok, Baron and François (1979), Wecharatana and Shah (1980), and Brown (1972), (after Bažant and Oh 1981).

The samples of test data available in the literature are sufficiently large for a statistical regression analysis of the errors. Fig. 11 shows a regression analysis of the maximum load data for twenty-two different concretes (30). In this plot, the abscissa is $X = P_t/P_0$ and the ordinate is $Y = P_m/P_0$, in which P_m = measured maximum load P_{max}, P_t = theoretical value of P_{max}, and P_0 = failure loads calculated according to the strength theory. If the theory were perfect, then the plot of Y vs. X would have to be a straight line of slope 1.0, passing through the origin. Thus, the vertical deviation of the data points from the regression line characterize the errors of the theory, and so do the deviations of the regression line slope from 1.0 and of its intercept from the origin. The coefficient of variation, ω, of the vertical deviation from the regression line in Fig. 11 was calculated to be

$$\begin{aligned} &\text{For the present fracture theory} && \omega = 0.066 \\ &\text{For linear fracture theory} && \omega = 0.267 \\ &\text{For strength criterion} && \omega = 0.650 \end{aligned} \tag{25}$$

These results confirm that the improvement achieved with the present nonlinear fracture theory is quite significant.

A similar statistical regression analysis has been carried out (30) for the test data available in the literature on the R-curves. In this regression analysis, the fracture energy values were normalized with regard to the product $f'_c\ d_a$, and the theoretical values of $\log (G_f/f'_c d_a)$ were plotted against the measured values of this ratio. Again, if everything worked perfectly, this plot would have to be a straight line of slope 1.0 and intercept 0.0. The standard errors for the vertical deviations from this regression line have been calculated, for the sets of various test data available in the literature,

$$\begin{aligned} &\text{For the present fracture theory:} && s = 0.083 \\ &\text{For linear fracture theory:} && s = 0.317 \end{aligned} \tag{26}$$

The values of the fracture energy obtained for the optimum fits of various fracture data on concrete were further examined to see whether the fracture energy could be approximately predicted from elementary characteristics of concrete. The following approximate formula was found:

$$G_f = (2.72 + 0.0214\ f'_c)\ f'^2_t\ d_a/E \tag{27}$$

in which f'_c must be in psi (psi = 6895 Pa), d_a = maximum aggregate size, E = elastic modulus. It must be emphasized, however, that Eq. 24 yields only the fracture energy values for the present nonlinear theory, and not the apparent fracture energy values determined according to linear fracture mechanics or those determined from other theories.

Further interesting problems arise for large structures for which finite elements whose size is 3-times the aggregate size would result in too many unknowns. In many such situations, e.g., concrete reactor vessels or dams, much larger finite elements have to be used. In such a case, it appears that the parameter of overriding importance is the value of the fracture energy, and that the declining slope of the stress-strain diagram and the value of the strength can be adjusted, for very large structures, so as to give the correct fracture energy value when a much larger finite element forms the crack band

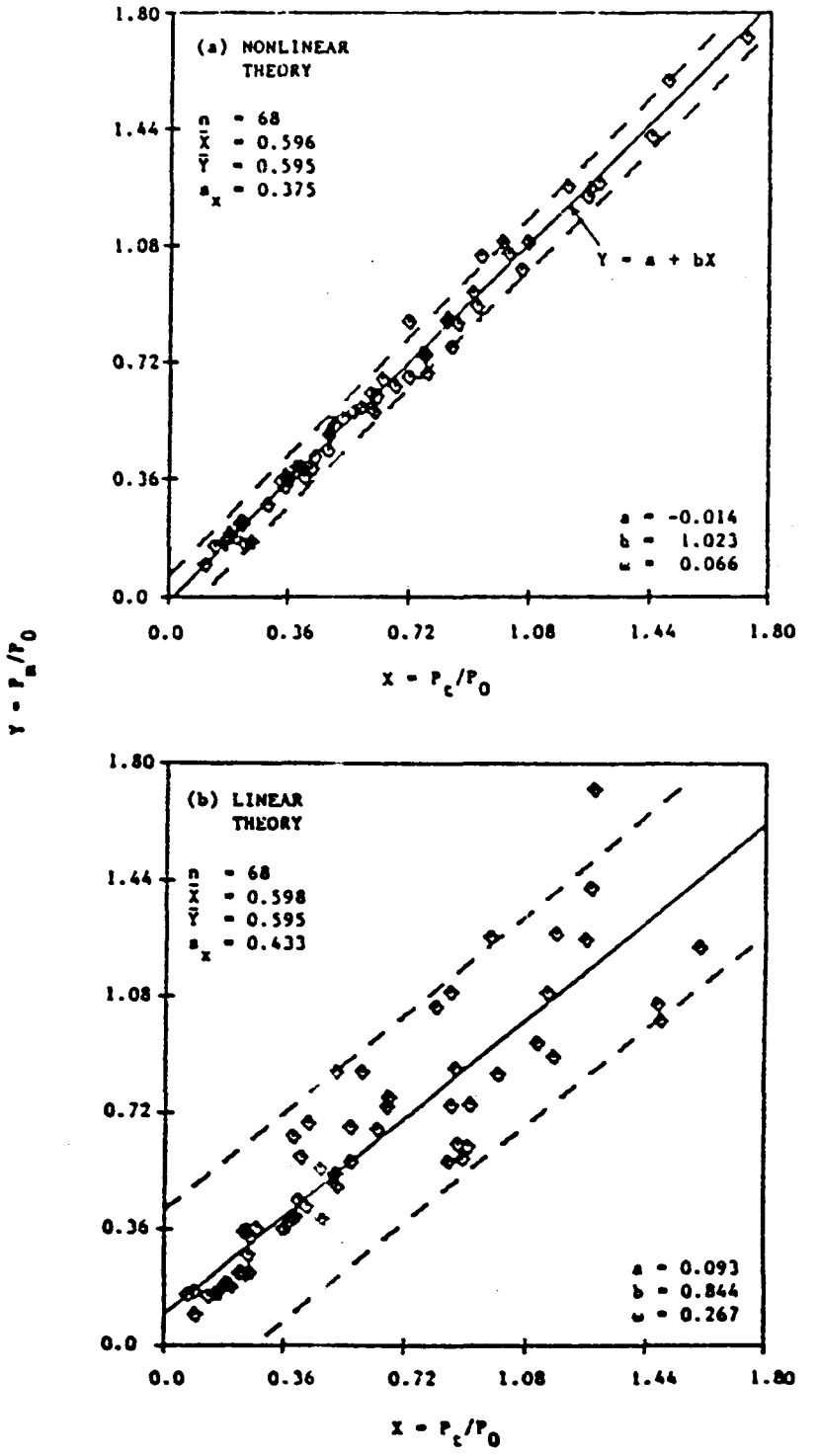

Fig. 11. Plot of Measured vs. Theoretical Values of Maximum Loads From Tests of Twenty-two Different Concretes Given in the Literature (after Bažant and Oh, 1981).

front. For this purpose, if the structure is very large, one may consider a sudden stress drop after a certain strength limit is reached. Occurance of the sudden stress drop must be determined either directly on the basis of an energy criterion for fracture formulated for a blunt crack band, or in terms of an adjusted strength limit, called the equivalent strength. For details see Ref. 30.

Further rather difficult questions arise when shear is superimposed on the crack planes, either during the progressive formation of microcracks or after the full fracture forms. In the first case, one must take into account the fact that superposition of the shear causes a rotation of the principal stress direction. One can then no longer use the total stress-strain relations, as we outlined above; rather one must use a tensorialy invariant incremental stress-strain relation. This problem has been discussed in Ref. 59 and an invariant form of a strain-softening stress-strain relation leading to a complete reduction of stress to 0 has been indicated.

For the second case, namely when shear is superimposed on completely formed-continuous cracks, one needs to formulate a stiffness matrix of a material taking into account the friction and dilatancy of these continuous cracks. Various forms of such matrices have been proposed, based either on the simple concept of friction or on more realistic, but also more complicated, stress-displacement relations observed in tests of cracked concrete specimens; see Ref. 59-60.

CONCLUSION

The internal mechanism of the inelastic behavior of concrete, characterized chiefly by progressive microcracking, crack friction and dilatancy lends us to formulate non-classical mathematical models for the constitutive behavior as well as fracture. Due to the large size of the heterogeneties in the microstructure (the pieces of aggregate), the distinction between constitutive models and fracture models is becoming blurred. Fracture aspects, consisting in unstable strain localization, cannot be forgotten in the formulation of constitutive equations which involve strain-softening, while fracture seems to be most reasonably approached by means of stress-strain relations for the fracture process zone.

ACKNOWLEDGMENT

Financial support under U. S. National Science Foundation Grant No. CEE-8009050 is greatefully appreciated. Mary Hill is thanked for her careful and prompt typing of the manuscript.

REFERENCES

1. ASCE Structural Division Committee on Finite Element Analysis of Reinforced Concrete Structures (chaired by A. Nilson), "Finite Element Analysis of Reinforced Concrete Structures," Chapt. 2, ASCE Special Publication, New York 1982.

2. Malvern, L. E., "Introduction to the Mechanics of a Continuous Medium," Prentice-Hall, Englewood, N.J., 1969.

3. Bažant, Z. P., "Critique of Orthotropic Models and Triaxial Testing of Concrete and Soils," Structural Engineering Report No. 79-10/640c, Northwestern University, Evanston, Ill., Oct. 1979; also in press, Journal of the Engineering Mechanics Division, ASCE.

4. Fung, Y. C., "Foundations of Solid Mechanics," (Chapter 6), Prentice Hall, Englewood Cliffs, N. J., 1975.

5. Bažant, Z. P., and Kim, S. S., "Nonlinear Creep of Concrete - Adaptation and Flow," J. of Eng. Mech. Div., ASCE, 105:429-446, 1979, (Proc. Paper 14654).

6. Bažant, Z. P., "Work Inequalities for Plastic-Fracturing Materials," Int. J. of Solids and Structures, 16:, 1980.

7. Dougill, J. W., "On Stable Progressively Fracturing Solids, ZAMP (Zeitschrift für Angewandte Mathematik und Physik), 1976, pp. 423-437.

8. Dougill, J. W., "Some Remarks on Path Independence in the Small in Plasticity," Quarterly of Appl. Math., 32: 1975, pp. 233-243.

9. Aschl, H., Linse, D., and Stoeckl, S., "Strength and Stress-Strain Behavior of Concrete under Multiaxial Compression and Tension Loading, 1976, Technical Report, Technical University, Munich, Germany.

10. Balmer, G. G., "Shearing Strength of Concrete under High Triaxial-Stress-Computation of Mohr's Envelope as a Curve," Structural Research Laboratory Report No. SP-23, 1949, Structural Research Laboratory, Denver, Colo.

11. Bresler, B., and Pister, K. S., "Strength of Concrete under Combined Stresses," Am. Concrete. Inst. J., 551, 1958, pp. 321-345.

12. Popovics. S., "A Numerical Approach to the Complte Stress-Strain Curves of Concrete," Cement and Concrete Research, 1973, pp. 583-599.

13. Kupfer, H. B., Hilsdorf, H. K., and Rüsch, H., "Behavior of Concrete under Biaxial Stresses," Am. Concrete Inst. J., 66, 1969, pp. 656-666.

14. Liu, T. C. Y., Nilson, A. H., and Slate, F. O., "Biaxial Stress-Strain Relations for Concrete," J. of Str. Div., ASCE, 98, 1972, pp. 1025-1034, (Proc. Paper 8905).

15. Shah, S. P., and Chandra, S., "Critical Stress, Volume Change and Micro-Cracking of Concrete," Am. Concrete Inst. J., 65, 1968, pp. 770-781.

16. Valanis, K. C., "A Theory of Viscoplasticity Without a Yield Surface," Archiwum Mechaniki Strossowanej (Archives of Mechanics, Warsaw) 23, 1971, pp. 517-551.

17. Schapery, R. A., "On a Thermodynamic Constitutive Theory and Its Application to Various Nonlinear Materials," Proc., IUTAM Symp, Kilbride, ed. B. A. Boley, Springer Verlag, New York, 1968.

18. Bažant, Z. P., "Endochronic Inelasticity and Incremental Plasticity, Int. J. of Solids and Structures, 14, 1968, pp. 691-714.

19. Bažant, Z. P., Bhat, P. D., Shieh, C. L., "Endochronic Theory for Inelasticity and Failure of Concrete Structures," Structural Engng. Report No. 76-12/259 (to Oak Ridge Nat. Lab.), Northwestern University, Evanston, Ill., Dec. 1976 (available from NTIS, Springfield, Va.)

20. de Villiers, I. P., "Implementation of Endochronic Theory for Analysis of Concrete Structures, " Ph.D. Dissertation, University of California, Berkeley, 1977.

21. Sørensen, S. I., Arnesen, A., Bergan, P. G., "Nonlinear Finite Element Analysis of Reinforced Concrete Using Endochronic Theory, Finite Elements in Nonlinear Mechanics," Proc. of Int. Conf. held at Geilo, Norway, 1977, Tapir, Norwegian Inst. of Tech., Trondheim, 1978, pp. 167-190.

22. SAMSON, "Computer Code for Dynamic Stress Analysis of Media-Structure Problems with Nonlinearities," IIT Research Inst., version by D. Seemann, et al, Air Force Weapons Lab INTES (J. Jeter's extension of T. B. Belytschko's program) 1980.

23. Hsieh, B. J., "On the Uniqueness and Stability of Endochronic Theory," Trans. of the ASME, J. of Applied Mechanics, Vol. 47, Dec. 1980, pp. 748-454.

24. Rivlin, R. S., "Some Comments on the Endochronic Theory of Plasticity," Report N. CAM-100-33, Center for the Application of Math., Lehigh Univ. Bethlehem PA; Int. J. of Solids and Structures, 1980.

25. Sandler, I. S., "On the Uniqueness and Stability of Endochronic Theories of Material Behavior, Trans. ASME, Series E, J. of Appl. Mech, 2978, pp. 263-266.

26. Bažant, Z. P., and Bhat, P., "Endochronic Theory of Inelasticity and Failure of Concrete," J. of Eng. Mech. Div., ASCE, 1977, pp. 701-722.

27. Bažant, Z. P. and Shieh, C. L., "Hysteretic Fracturing Endochronic Theory for Concrete," Proc. ASCE, J. of the Engng. Mechanics Div., Vol. 106, No. EM5, Oct. 1980, pp. 929-950, and Aug. 1981, p. 728.

27a. Drucker, D. C., "A Definition of Stable Inelastic Material," J. Appl. Mech., ASME, 26, 1959, pp. 101-106.

28. Drucker, D. C., and Prager, W., "Soil Mechanics and Plastic Analysis or Limit Design, Quarterly of Appl. Math., 10, 1952, pp. 157-165.

29. Mandel, J., "Conditions de Stabilité et Postulat de Drucker, In: Rheology and Soil Mechanics, held in Grenoble, 1964; ed. by J. Kravtchenko and P. M. Sirieys, Springer Verlag, Berlin, 1966, pp. 58-68. (IUTAM Symp.)

30. Bažant, Z. P., Oh, B. H., "Concrete Fracture via Stress-Strain Relations," Report No. 81-10/665c, Center for Concrete and Geomaterials, Northwestern University, Evanston, Illinois, USA, 1981.

31. Suidan, M., and Schnobrich, W. C. "Finite Element Analysis of Reinforced Concrete," Journal of the Structural Division, ASCE, Vol. 99, No. ST10, Oct. 1973, pp. 2109-2122.

32. Evans, R. H., and Marathe, M. S. "Microcracking and Stress-Strain Curves for Concrete in Tension," Matériaux et Constructions, Vol. 1, No. 1, 1968, pp. 61-64.

33. Barenblatt, G. I., "The Formation of Equilibrium Cracks During Brittle Fracture. General Ideas and Hypothesis. Axially-Symmetric Cracks," Prikladnaya Matematika i Mekhanika, Vol. 23, No. 3, 1959, pp. 434-444.

34. Kfouri, A. P., and Miller, K. J., "Stress Displacement, Line Integral and Closure Energy Determinations of Crack Tip Stress Intensity Factors," Int. Journal of Pres. Ves. and Piping, Vol. 1, No. 3, 1974, pp. 179-191.

35. Knauss, W. G., "On the Steady Propagation of a Crack in a Viscoelastic Sheet; Experiments and Analysis," Reprinted from The Performation in Fracture of High Polymers, Ed. by H. H. Kauseh, Publ. Plenum Press, 1974, pp. 501-541.

36. Wnuk, M. P. "Qasi-Static Extension of a Tensile Crack Contained in Viscoelastic Plastic Solid," Journal of Applied Mechanics, ASME, Vol. 41, No. 1, 1974, pp. 234-248.

37. Kfouri, A. P., and Rice. J. R., "Elastic/Plastic Separation Energy Rate for Crack Advance in Finite Growth Steps," in "Fracture 1977" (Proc. of the 4th Intern. Conf. on Fracture, held in Waterloo, Ontario); Ed. by D. M. R. Taplin, University of Waterloo Press, Vol. 1, 1977, pp. 43-59.

38. Hillerborg, A., Modéer, M., and Petersson, P. E., "Analysis of Crack Formation and Crack Growth in Concrete by Means of Fracture Mechanics and Finite Elements," Cement and Concrete Research, Vol. 6, 1976, pp. 773-782.

39. Petersson, P. E., "Fracture Energy of Concrete: Method of Determination," Cement and Concrete Research, Vol. 10, pp. 78-89, and "Fracture Energy of Concrete: Practical Performance and Experimental Results," Cement and Concrete Research, Vol. 10, 1980, pp. 91-101.

40. Bažant, Z. P. and Cedolin, L. "Blunt Crack Band Propagation in Finite Element Analysis," Journal of the Engineering Mechanics Division, ASCE, Vol. 105, No. EM2, Proc. Paper 14529, 1979, pp. 297-315.

41. Bažant, Z. P., and Cedolin, L., "Fracture Mechanics of Reinforced Concrete," Journal of the Engineering Mechanics Division, ASCE, Vol. 106, No. EM6, Proc. Paper 15917, 1980, pp. 1287-1306.

42. Kaplan, M. F., "Crack Propagation and the Fracture of Concrete," American Concrete Institute Journal, Vol. 58, No. 11, Nov. 1961.

43. Kesler, C. E., Naus, D. J., and Lott, J. L., "Fracture Mechanics — Its Applicability to Concrete," International Conference on the Mechanical Behavior of Materials, Koto, Aug. 1971.

44. Naus, D. J., "Applicability of Linear-Elastic Fracture Mechanics to Portland Cement Concretes," Thesis Submitted in Partial Fullfillment of the Requirements for the Degree of Doctor of Philosophy, University of Illinois at Urbana-Chaimpaign, 1971.

45. Mindess, S., Lawrence, F. V., and Kesler, C. E., "The J-Integral As a Fracture Criterion for Fiber Reinforced Concrete," Cement and Concrete Research, Vol. 7, 1977, pp. 731-742.

46. Shah, S. P., and McGarry, F. J., "Griffith Fracture Criterion and Concrete," Journal of the Engineering Mechanics Division, ASCE, Vol. 97, No. EM6, Proc. Paper 8597, 1971, pp. 1662-1676.

47. Brown, J. H., "Measuring the Fracture Toughness of Cement Paste and Mortar," Magazine of Concrete Research, Vol. 24, No. 81, Dec. 1972, pp. 185-196.

48. Entov, V. M., and Yagust, V. I., "Experimental Investigation of Laws Governing Quasi-Static Development of Macrocracks in Concrete," Mechanics of Solids, (translation from Russian), Vol. 10, No. 4, 1975, pp. 87-95.

49. Gjørv, O. E., Sørensen, S. I., and Arnesen, A., "Notch Sensitivity and Fracture Toughness of Concrete," Cement and Concrete Research, Vol. 7, 1977, pp. 333-344.

50. Huang, C.M.J., "Finite Element and Experimental Studies of Stress Intensity Factors for Concrete Beams," Thesis Submitted in Partial Fulfullment of the Requirements for the Degree of Doctor of Philosophy, Kansas State Univeraity, Kansas, 1981.

51. Sok, C., Baron, J., and Francois, D., "Mecanique de la Rupture Appliquee au Béton Hydraulique," Cement and Concrete Research, Vol. 9, 1979, pp. 641-648.

52. Swartz, S. E., Hu, K. K., Fartash, M., and Huang, C.M.J., "Stress Intensity Factors for Plain Concrete in Bending - Prenotched Versus Precracked Beams," Report, Department of Civil Engineering, Kansas State University, Kansas, 1981.

53. Wecharatana, M., and Shah, S. P., "Resistance to Crack Growth in Portland Cement Composites," Report, Department of Material Engineering, University of Illinois at Chicago Circle, Chicago, Ill., 1980.

54. Carpinteri, A., "Static and Energetic Fracture Parameters for Rocks and Concretes," Report, Istituto di Scienza delle Costruzioni-Ingegneria, University of Bologna, Italy, 1980.

55. Carpinteri, A., "Experimental Determination of Fracture Toughness Parameters K_{IC} and J_{IC} for Aggregative Materials," Advances in Fracture Research," (Proc, 5th International Conference on Fracture, Cannes, France), 1981: Ed. by D. Francois, Vol. 4, pp. 1491-1498.

56. Walsh, P. F., "Fracture of Plain Concrete," The Indian Concrete Journal, Vol. 46, No. 11, 1979, pp. 469, 470, and 476.

57. Carpinteri, A., "Static and Energetic Fracture Parameters for Rocks and Concretes," Report, Istituto di Scienza della Costruzioni-Ingegneria, University of Bologna, Italy, 1980.

58. Bažant, Z. P., "Crack Band Model for Fracture of Geomaterials," Proceedings, 4th Intern. Conf. on Numerical Methods in Geomechanics, ed. by Z. Eisenstein, Edmonton, Alberta, Canada, Vol. 3, 1982.

59. Bažant, Z. P., and Gambarova, P., "Rough Cracks in Reinforced Concrete," J. Str. Div., ASCE, 1980, pp. 819-842.

60. Bažant, Z. P., and Tsubaki, T., "Slip-Dilatancy Model for Cracked Reinforced Concrete," J. of Str. Div., ASCE, 1980.